



Short communication

Solid oxide fuel cell bi-layer anode with gadolinia-doped ceria for utilization of solid carbon fuel

Isaiah D. Kellogg^{a,b,*}, Umit O. Koylu^a, Fatih Dogan^b^a Department of Mechanical and Aerospace Engineering, Missouri University of Science and Technology, 290A Toomey Hall, 400 West 13th Street, Rolla, MO 65409, USA^b Department of Materials Science and Engineering, Missouri University of Science and Technology, 223 McNutt Hall, 1400 N. Bishop, Rolla, MO 65409, USA

ARTICLE INFO

Article history:

Received 7 April 2010

Received in revised form 27 May 2010

Accepted 27 May 2010

Available online 1 June 2010

Keywords:

Solid oxide fuel cell

YSZ

Gadolinia-doped ceria

Anode

Soot

Carbon

ABSTRACT

Pyrolytic carbon was used as fuel in a solid oxide fuel cell (SOFC) with a yttria-stabilized zirconia (YSZ) electrolyte and a bi-layer anode composed of nickel oxide gadolinia-doped ceria (NiO–GDC) and NiO–YSZ. The common problems of bulk shrinkage and emergent porosity in the YSZ layer adjacent to the GDC/YSZ interface were avoided by using an interlayer of porous NiO–YSZ as a buffer anode layer between the electrolyte and the NiO–GDC primary anode. Cells were fabricated from commercially available component powders so that unconventional production methods suggested in the literature were avoided, that is, the necessity of glycine–nitrate combustion synthesis, specialty multicomponent oxide powders, sputtering, or chemical vapor deposition. The easily-fabricated cell was successfully utilized with hydrogen and propane fuels as well as carbon deposited on the anode during the cyclic operation with the propane. A cell of similar construction could be used in the exhaust stream of a diesel engine to capture and utilize soot for secondary power generation and decreased particulate pollution without the need for filter regeneration.

© 2010 Elsevier B.V. All rights reserved.

1. Introduction

Solid oxide fuel cells (SOFC) are capable of directly converting chemical energy from a wide variety of liquid and gaseous fuels into electrical energy. The high temperature necessary to enable oxygen ion diffusion through the ceramic electrolyte makes even the direct use of solid carbon fuel possible [1,2]. Solid carbon may come from internal pyrolysis of hydrocarbon fuel or as soot from the exhaust gas of an internal combustion engine. Diesel engine exhaust soot has been removed from an exhaust filter with an electrochemical reaction [3] but it may be possible to recover energy rather than expend energy while consuming the unwanted soot particulate pollution, similar to carbon particulate filter regeneration downstream from thermal partial oxidation reformers intended to feed hydrogen to a SOFC [4]. SOFCs capable of using solid carbon fuel could recover a significant amount of unused energy while simultaneously decreasing particulate pollution from diesel engine exhaust stream. The amount of electricity recovered from this soot can reduce the load on the alternator and remove the need for filter regeneration, both of which would increase fuel efficiency.

Utilization of solid carbon fuel may be by direct oxidation or by Boudouard gasification [5], which are both made more practical by the correct choice of anode material to catalyze the carbon oxidation reaction [5–7], which in turn makes hydrocarbon fuels more practical by oxidizing the deposited solid carbon before it builds up to the point of hindering cell performance.

An SOFC requires the use of an ion conducting ceramic both as the electrolyte and as one component of a cermet anode. High ionic conductivity is necessary to allow oxygen ion transport and minimize internal cell resistance, and for the electrolyte a low electronic conductivity is necessary to minimize electron leakage. When the ion conductor is used as part of the anode cermet, it should also have high catalytic activity toward oxidation of the selected fuel.

Two ceramic materials commonly used as ion conductors in SOFCs are yttria-stabilized zirconia (YSZ) and gadolinia-doped ceria (GDC). GDC is more catalytically active than YSZ, performing more than eight times better as a catalyst for oxidation of solid carbon than does YSZ [8], and the reaction zone in a GDC anode extends significantly beyond the three-phase boundary [9]. These characteristics make GDC more favorable as the anode ion conductor for the use of solid carbon fuel in a SOFC [5,10]. YSZ provides the low electrical conductivity which is desirable in an electrolyte material, but as an anode material suffers from lower catalytic activity for fuel oxidation than ceria. GDC has higher ionic conductivity than YSZ but suffers from higher electronic conductivity, which makes it less suitable for use as an electrolyte; however YSZ has been used

* Corresponding author at: Department of Mechanical and Aerospace Engineering, Missouri University of Science and Technology, 290A Toomey Hall, 400 West 13th Street, Rolla, MO 65409-0050, USA. Tel.: +1 573 341 6601; fax: +1 573 341 4607.

E-mail address: ikellogg@mst.edu (I.D. Kellogg).

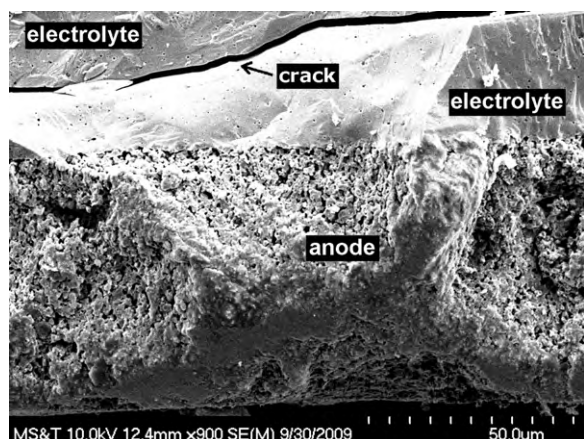


Fig. 1. YSZ electrolyte (top) and Ni/GDC anode (bottom) showing voids and a crack.

as a thin layer to block electronic conduction with a GDC electrolyte [11].

An SOFC composed of a YSZ electrolyte combined with a GDC anode would have less electron leakage and higher catalytic activity. GDC also shows increased electronic conductivity in the low oxygen partial pressure environment of the anode, further decreasing anode resistance. However, when GDC and YSZ are sintered as adjacent layers, there are significant chemical compatibility problems [12], including excessive diffusion of Y ions into the GDC causing bulk shrinkage and voids which lead to decreased overall cross-sectional area and lower ionic conductivity, as well as lower mechanical strength. Adding Ni to the anode somewhat suppresses the undesirable solid-state reaction [13], but does not eliminate the problem, as illustrated in Fig. 1, which shows voids and a crack caused by a Ni/GDC anode sintered onto a YSZ electrolyte. An interlayer of $\text{Ce}_{0.43}\text{Zr}_{0.43}\text{Gd}_{0.10}\text{Y}_{0.04}\text{O}_{1.93}$ can be used to slow the solid-state reaction so a GDC anode can be sintered onto a YSZ electrolyte [13] but this cannot be done with commercially available materials, requiring combustion synthesis or other unconventional methods.

Previous cell construction using GDC anode directly applied to the YSZ electrolyte revealed several problems after sintering, consistent with results from other groups [12,13]. Excess diffusion of Y from the YSZ electrolyte into the GDC anode caused void formation and bulk shrinkage, which in turn led to subsurface cracking. Fig. 2a shows the surface of the electrolyte after the anode flaked off. Fig. 2b shows some of the anode flakes on both the front anode surface and the rear where a thin layer of electrolyte is still visible.

Commercial cells with a YSZ electrolyte and GDC anode are available and do well in testing, both in terms of power pro-

Table 1
Anode compositions by weight.

Layer	NiO (wt%)	YSZ (wt%)	GDC (wt%)
Anode 1	60	40	0
Anode 2	55	15	30

duction and resistance to carbon fouling [6], while experimental cells of similar composition have successfully used solid carbon as fuel [10]. However, few researchers have discussed the methods used to overcome the difficulties in applying a GDC anode to a YSZ electrolyte. The methods which have been presented are less than completely effective or require specialty multicomponent oxide materials or unconventional synthesis methods such as glycine–nitrate combustion synthesis [13]. The first objective of this paper is to present a simple and effective method to fabricate a functional SOFC using a GDC cermet anode and a YSZ electrolyte using only the commercially available oxide powders necessary to make either a YSZ or a GDC based anode. The second objective is to successfully demonstrate the utilization of not only hydrogen and a hydrocarbon fuel but also solid carbon fuel and this bi-layer SOFC anode for their applications in power generation and pollution control.

2. Experimental methods

2.1. Fabrication

Several cells were fabricated for testing. Electrolytes were 300 μm thick, fully-dense 8 mol% Y_2O_3 stabilized zirconia (8YSZ) disks tape cast from Tosoh TZ-8Y powder. In order to promote oxidation of solid carbon as well as increase anode conductivity, GDC was chosen as the ionic conductor for the anode. Two anode inks were prepared, denoted as Anode 1 and Anode 2. Each anode ink was mixed from commercial off-the-shelf component powders; NiO (Aldrich, USA), GDC (Praxair, USA), and YSZ (TZ-8Y, Tosoh, Japan); then combined with an equal amount by weight of Ferro B-75000, a commercial pre-prepared screen printing binder, and mixed in mortar and pestle. Anode compositions are given in Table 1 by weight percent according to industry standard.

Anode 1 ink was first painted onto an electrolyte disk and allowed to dry at room temperature. Anode 2 ink was then painted over Anode 1 and also allowed to dry at room temperature. The anodes were then sintered in air at 1350 $^\circ\text{C}$ for 4 h, resulting in a sintered anode with a thickness of between 25 and 30 μm , as measured with SEM micrography.

This anode fabrication method is much simpler or less expensive than many of the methods mentioned in the literature. No combustion synthesis or chemical vapor deposition was necessary, and

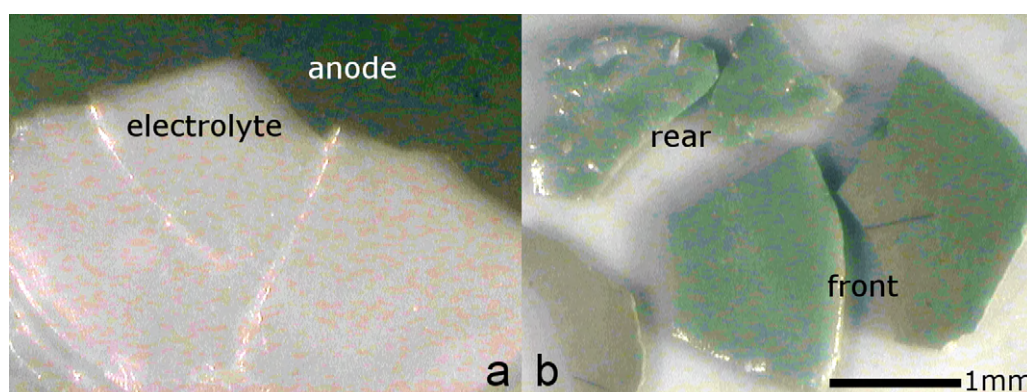


Fig. 2. (a) YSZ electrolyte surface after GDC anode flaked off; (b) GDC anode flakes showing a thin layer of electrolyte remaining on the rear surface.

no equipment more complicated than a simple sintering furnace was used for fabrication. Commercial samples by this method could be manufactured with a simple screen printing or inkjet process, which would be both simpler and much less expensive than vapor deposition, while laboratories can make effective fuel cell samples without the cost of specialty multicomponent oxides.

Cathode ink was prepared by combining $\text{La}_{0.8}\text{Sr}_{0.2}\text{Fe}_{0.8}\text{Co}_{0.2}$ oxide powder with the same screen printing binder and mixing in mortar and pestle. The cathode was painted onto each electrolyte disk opposite the anode and sintered in air at 900°C for 1 h.

2.2. Test procedures

Cells were mounted in a furnace and heated to 800°C at a rate of 5°Cmin^{-1} , and all measurements were taken at this furnace temperature. The actual cell temperature was $5\text{--}15^\circ\text{C}$ higher due to the exothermic reactions taking place at the electrodes. The actual temperature increase depended on the type of test being performed. The cathode was exposed to a flow of preheated air at 300 mL min^{-1} , and the anode was exposed to various preheated fuel gases at 300 mL min^{-1} , including $5\%\text{ H}_2$ in Ar, $10\%\text{ H}_2$ in N_2 , and propane. All gas flows unless otherwise specified were at a rate of 300 mL min^{-1} . When operated with propane fuel, solid carbon was deposited on the anode by pyrolysis of the propane. Any remaining fuel gas was flushed from the test chamber with Ar for sufficiently long times to ensure no gaseous fuels remained in the system [8,5]. The solid carbon remaining on the anode was used as indirect fuel by flowing CO_2 gas, which is a major component of hydrocarbon combustion exhaust and found with soot in diesel engine exhaust, over the anode to gasify the carbon via the Boudouard reaction, converting it to CO which can be directly utilized by the anode as fuel, according to $\text{C} + \text{CO}_2 \rightarrow 2\text{CO}$.

Temperature measurements were taken with a type R thermocouple. Gas flow was measured with Cole-Parmer 112-02-N ball flow meters calibrated for nitrogen. Correction factors for the ball flow meters were determined by flowing gas through a Tylan FC-260 electronic mass flow controller and then through the ball flow meters. Electrical tests were taken by four-point probe with a Solartron CellTest 1470 system, and recorded by CorrWare and Zplot software. Impedance was measured from 1 Hz to 1×10^6 Hz at an amplitude of 20 mV AC. Voltage measurements are accurate to within 1%, current density and impedance measurements to within 5%, for a 95% confidence interval. SEM micrography was performed with a Hitachi S-4700 scanning electron microscope.

3. Results and discussion

3.1. Electron microscopy

A representative sample SOFC identical to the ones used in these tests was fractured and examined under SEM. Fig. 3 shows the cross-section, with a thin porous bi-layer anode on the bottom firmly bonded to the dense electrolyte on the top of each picture, revealing that the electrolyte is intact and has no voids. If detrimental interactions between the GDC and YSZ had occurred, there would be significant bulk shrinkage evidenced by voids or cracking in the electrolyte layer near the porous anode, as shown in Fig. 1. The adjacency of the GDC and YSZ is located in the anode, where porosity is necessary for gas transport, and where bulk shrinkage normally takes place during sintering.

3.2. Electrical tests

Fig. 4 shows the results of the open circuit voltage (OCV) tests with the anode exposed to various fuels, including $5\%\text{ H}_2$ in Ar and $10\%\text{ H}_2$ in N_2 , which produce identical voltage around 1.0V, both

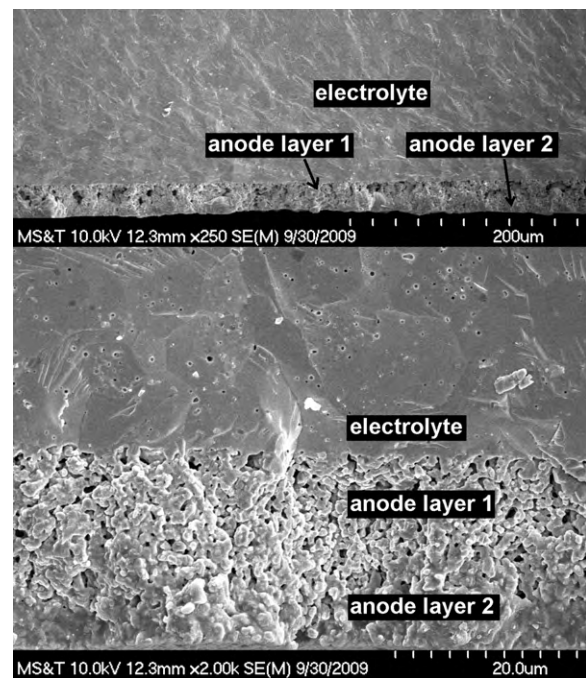


Fig. 3. SEM photos of the SOFC cross-section showing the anode and proximate electrolyte.

represented on trace (a), revealing that the SOFC was capable of producing about 1 V in hydrogen which is consistent with the value predicted by the Nernst equation. Trace (b) in Fig. 4 shows the OCV as the cell is first exposed to propane after operating with H_2 fuel, and trace (c) shows the voltage in propane after an hour of propane operation and then 300 s of potentiostatic operation at 0.5 V, which allows oxide ion current to flow through the electrolyte and consume the solid carbon which clogged the anode porosity. Trace (d) shows the voltage recorded when the gas was switched to argon at 0 s, after 420 s of open circuit operation in propane to pyrolytically deposit solid carbon on the anode.

It is interesting to note that after operating the sample in propane for <60 s, the OCV had dropped by about 0.075 V from its initial value, but after increasing the current and operating in potentiostatic mode at 0.5 V, the voltage increased initially, but slowly decreased again. This is consistent with results from other groups [5] that the open circuit condition tends to allow carbon

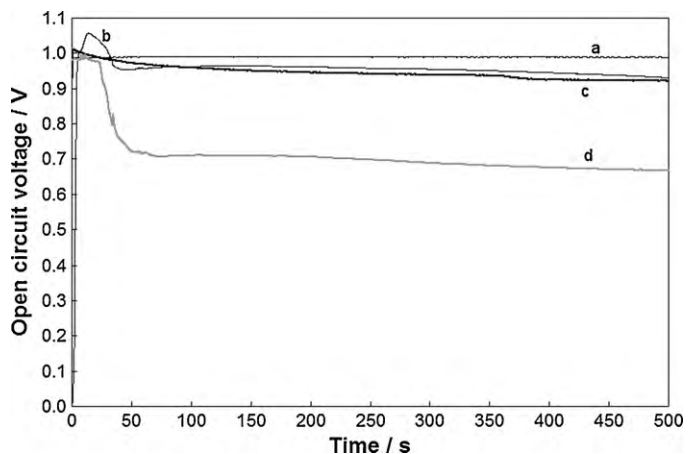


Fig. 4. OCV of the SOFC when operated with (a) $5\%\text{ H}_2$ and $10\%\text{ H}_2$ (b) initial propane, (c) propane after 1 h of propane and 5 min of potentiostatic operation at 0.5 V, (d) Ar after 7 min of propane on a new cell.

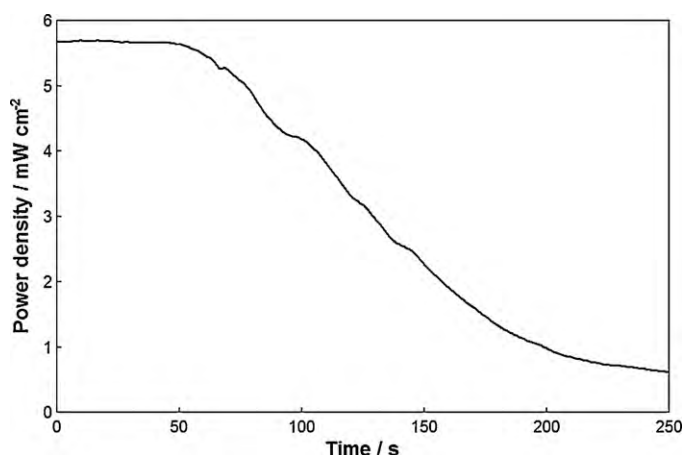


Fig. 5. Area specific power of cell in operation with CO₂ over anode after 7 min OCV operation in propane and 10 min Ar flush.

build-up which decreases the OCV, while an increased current consumes some of the deposited carbon and restores some porosity to the anode, restoring the high OCV.

The cell initially produced a maximum power of about 65.6 mW cm⁻² using 5% H₂ as fuel, but after about an hour the cell had degraded slightly and only produced 61.6 mW cm⁻² with 10% H₂ fuel, and subsequently 61.8 mW cm⁻² with propane fuel. This amount of power is lower than current thin-electrolyte technology cells, but it is quite respectable when the thicker 300 μm electrolyte is taken into account.

A new identical cell was exposed to propane fuel gas stream at 300 mL min⁻¹ for 420 s, achieving identical voltage performance to (b) in Fig. 4, co-represented by trace (b). The cell was then flushed with pure Ar at 300 mL min⁻¹ as seen in (d) of Fig. 4. The voltage stayed nearly constant at about 1 V for several seconds until the gas tubes had been flushed of propane, and then abruptly dropped as the propane was flushed away from the cell. By 100 s after the gases had been switched, the voltage had leveled and stayed about the same for a further 600 s. This shows that the propane is certain to have been removed from the cell in only a few minutes. The anode gas was then switched to CO₂ under which the cell generated >0.85 V for 2 min after the Ar had been flushed away. Therefore the cell was capable of voltage generation using pyrolytically deposited carbon as fuel, in both Ar and CO₂ gases.

After an identical carbon-deposition and argon flush, current was recorded while the cell was held at 0.4 V, approximately half the OCV which was recorded with CO₂ gas flow over the pyrolytically deposited carbon. The cell produced a current density >14 mA cm⁻² and power of 5.65 mW cm⁻² for about 60 s, before the soot started to become depleted, as seen in Fig. 5. Although the power generated with solid carbon fuel is much lower than that generated with hydrogen or hydrocarbon fuels, it is consistent with the early results of other groups [8], and is a reasonable value for the first fabrication of this type of cell. Subsequent tests can be expected to increase power by varying the anode thicknesses, composition, porosity, or sintering schedules.

The linear slope of the decrease from 75 to 175 s is probably the result of the consumption of carbon at the most active areas of the anode first, those areas of three-phase boundary closest to the electrolyte [5]. As the carbon closest to the electrolyte was consumed, oxygen ions were required to travel a longer distance through the ionic conductor in the anode to gain proximity to fuel at a three-phase boundary. This longer ionic conduction distance increased the overpotential and decreased the power. However, recent studies indicate that little pyrolytic carbon is deposited on the more active interior portions of the anode [14], so a more important

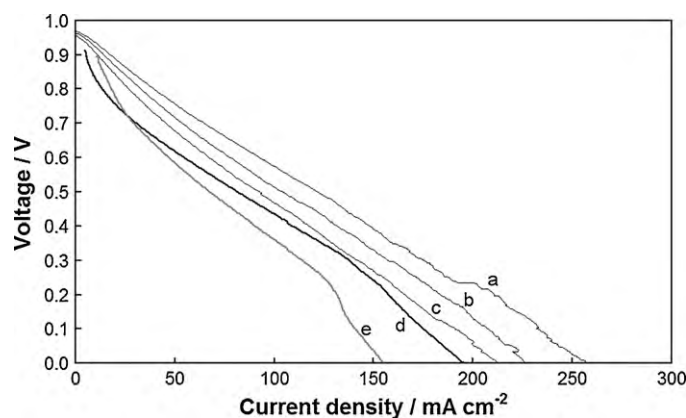


Fig. 6. Polarization graph of three subsequent tests in 5% H₂ (a–c) and two subsequent tests in propane (d and e).

aspect may be that the generation point of the CO gas moved farther away from the electrolyte, further increasing the overpotential due to gas transport issues. The effect of increasing conduction distance and the effect of increased gas transport distance would both be expected to decrease the produced power in a linear fashion.

Two more subsequent tests showed near identical performance, with only minor decrease attributable to electrolyte aging, indicating that at least three short 10-min deposition/utilization cycles are possible. Although longer testing times and more deposition/utilization cycles may reveal anode deterioration, longevity can be improved in subsequent tests by varying anode thickness, porosity, and particle size. The results presented in this paper indicate that this simply fabricated cell is capable of power generation with a variety of fuels, including hydrocarbons and solid carbon, on par with cells fabricated by means of more elaborate and expensive methods.

The polarization profile shown in Fig. 6 reveals fairly ohmic behavior, which shows that the reactions at the anode and cathode do not excessively hinder the cells operation. Excess porosity or cracking in the electrolyte, such as from a YSZ–GDC interaction, would exhibit in the polarization profile as a decrease in voltage at higher current density due to an increased electrolyte overpotential. From (a) to (e) was about 6 h of operation of a single cell. A small decrease in voltage at higher current density is evident in (e), however the Cole–Cole impedance plot in Fig. 7 shows that this increase in overpotential is from the anode and is due to carbon build-up, which limited gas transport to the active area of the anode.

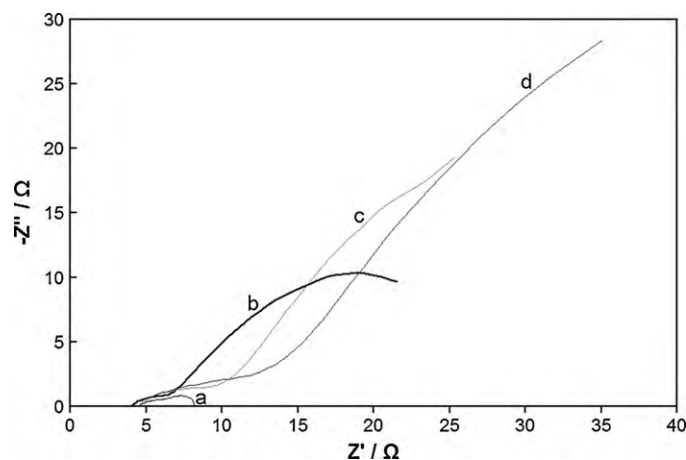


Fig. 7. Cole–Cole plot showing the impedance of the SOFC in operation with propane fuel after (a) 1 h, (b) 4 h, (c) 6 h, and (d) 8 h.

The Cole–Cole plot showing the impedance of the SOFC in operation is shown in Fig. 7 for four tests spanning about 8 h of operation in heavily-sooting propane. The first test is labeled (a), the fourth test is (b), the sixth (c) and the eighth test is labeled (d). Each test was about an hour apart, during which time other tests were run, including OCV and potentiostatic tests.

It should be noted that the electrolyte resistance (the distance on the Z' axis between the 0 mark and the intersection of the impedance curve with the Z' axis) remains fairly constant over the course of 4 h, only slightly decreasing from 5 to 4.5. This is attributable to aging of the electrolyte as it allows more electron leakage that decreases both the cell resistance and the OCV, as noted in Fig. 2. The cathode equivalent resistance (the size of the leftmost semicircle of the impedance curve) remains approximately the same as well. However, the anode equivalent resistance (size of the rightmost semicircle) increases dramatically from (a) to (d). This is because the anode overpotential increases as the anode becomes clogged with solid carbon, increasing the resistance of gas transport to the active area of the anode.

4. Conclusions

A simple method for applying a GDC bearing anode to a YSZ electrolyte was demonstrated, and power in excess of 60 mW cm^{-2} was recorded with both hydrogen fuel and propane fuel, and a reasonable power was recorded with pyrolytically deposited carbon fuel. Cell performance indicated no detrimental effects of YSZ/GDC adjacency, and SEM revealed no voids or other indications of the problems typical of YSZ/GDC interactions. The method presented in this paper is significantly simpler than the methods which rely on complex oxide mixtures, and more effective than the methods

which rely on higher Ni content in the GDC anode. This allows for easier fabrication of carbon-deposition resistant cells or cells which can collect and utilize soot from a diesel engine exhaust stream to decrease particulate pollution and increase fuel efficiency both by removing the necessity of filter regeneration and by secondary power generation which can decrease the power consumption requirements of the alternator.

Acknowledgement

The authors would like to thank the US Department of Education GAANN fellowship for financial support of this research.

References

- [1] S. Park, J.M. Vohs, R.J. Gorte, *Lett. Nat.* 404 (2000) 265–267.
- [2] D. Cao, Y. Sun, G. Wang, *J. Power Sources* 167 (2007) 250–257.
- [3] H. Christensen, J. Dinesen, H.H. Engell, K.K. Hansen, *Soc. Auto. Eng.* (1999), 1999-01-0472.
- [4] A. Raimondi, D. Fino, G. Saracco, *J. Power Sources* 193 (2009) 338–341.
- [5] S. Hasegawa, M. Ihara, *J. Electrochem. Soc.* 155 (2008) B58–B63.
- [6] P. Hofmann, A. Schweiger, L. Fryda, K.D. Panopoulos, U. Hohenwarther, J.D. Bentzen, J.P. Ouweltjes, J. Ahrenfeldt, U. Henriksen, E. Kakaras, *J. Power Sources* 173 (2007) 357–366.
- [7] T.J. Huang, C.H. Wang, *J. Power Sources* 163 (2006) 309–315.
- [8] M. Ihara, K. Matsuda, H. Sato, C. Yokoyama, *Solid State Ionics* 175 (2004) 51–54.
- [9] T. Nakamura, K. Yashiro, A. Kamai, T. Otake, K. Sato, T. Kawada, J. Mizusaki, *J. Electrochem. Soc.* 155 (2008) B1244–B1250.
- [10] M. Ihara, S. Hasegawa, *J. Electrochem. Soc.* 153 (2006) A1544–A1546.
- [11] Q.L. Liu, K.A. Khor, S.H. Chan, X.J. Chen, *J. Power Sources* 162 (2006) 1036–1042.
- [12] T.L. Nguyen, K. Kobayashi, T. Honda, Y. Iimura, K. Kato, A. Neghisi, K. Nozaki, F. Tappero, K. Sasaki, H. Shirahama, K. Ota, M. Dokiya, T. Kato, *Solid State Ionics* 174 (2004) 163–174.
- [13] A. Tsoga, A. Gupta, A. Naoumidis, P. Nikolopoulos, *Acta Mater.* 48 (2000) 4709–4714.
- [14] X.Y. Zhao, Q. Yao, S.Q. Li, N.S. Cai, *J. Power Sources* 185 (2008) 104–111.